Molecular Identification and Physiological Characterization of a Novel Monosaccharide Transporter from *Arabidopsis* Involved in Vacuolar Sugar Transport [W]

Alexandra Wormit,[a] Oliver Trentmann,[a] Ingmar Feifer,[a] Christian Lohr,[b] Joachim Tjaden,[a] Stefan Meyer,[c] Ulrike Schmidt,[c] Enrico Martinoia,[c] and H. Ekkehard Neuhaus[a,1]

[a] Pflanzenphysiologie, Technische Universität Kaiserslautern, D-67653 Kaiserslautern, Germany
[b] Zelluläre Neurobiologie, Technische Universität Kaiserslautern, D-67653 Kaiserslautern, Germany
[c] Institut für Pflanzenbiologie, Universität Zürich, CH-8008 Zürich, Switzerland

The tonoplast monosaccharide transporter (TMT) family comprises three isoforms in *Arabidopsis thaliana*, and TMT–green fluorescent protein fusion proteins are targeted to the vacuolar membrane. *TMT* promoter–β-glucuronidase plants revealed that the *TONOPLAST MONOSACCHARIDE TRANSPORTER1* (*TMT1*) and *TMT2* genes exhibit a tissue- and cell type–specific expression pattern, whereas *TMT3* is only weakly expressed. *TMT1* and *TMT2* expression is induced by drought, salt, and cold treatments and by sugar. During cold adaptation, *tmt* knockout lines accumulated less glucose and fructose compared with wild-type plants, whereas no differences were observed for sucrose. Cold adaptation of wild-type plants substantially promoted glucose uptake into isolated leaf mesophyll vacuoles. Glucose uptake into isolated vacuoles was inhibited by NH_4^+, fructose, and phlorizin, indicating that transport is energy-dependent and that both glucose and fructose were taken up by the same carrier. Glucose import into vacuoles from two cold-induced *tmt1* knockout lines or from triple knockout plants was substantially lower than into corresponding wild-type vacuoles. Monosaccharide feeding into leaf discs revealed the strongest response to sugar in *tmt1* knockout lines compared with wild-type plants, suggesting that TMT1 is required for cytosolic glucose homeostasis. Our results indicate that TMT1 is involved in vacuolar monosaccharide transport and plays a major role during stress responses.

INTRODUCTION

In plants, sugars fulfill essential functions as a main energy source, as substrates for polymer synthesis, as transport and storage compounds, or as carbon precursors required for a wide number of anabolic and catabolic reactions. In most plant species, sugars are present mainly in the form of the disaccharide sucrose or as glucose and fructose representing the major monosaccharides (ap Rees, 1994).

Long-distance transport of sugars in plants connects source and sink organs and occurs in the phloem sieve cells (Ruiz-Medrano et al., 2001). By contrast, short-distance transport into a plant cell occurs either symplastically through plasmodesmata or apoplastically via highly specific, monosaccharide or disaccharide transport proteins energized by proton symport (Ward et al., 1998; Bush, 1999; Williams et al., 2000). *Arabidopsis thaliana* possesses >60 putative isoforms of monosaccharide transporters separated in various clades (Lalonde et al., 2004), and 14 of these proteins represent the well-characterized plasma membrane–located hexose carrier group STP (Büttner and Sauer, 2000). In addition, *Arabidopsis* harbors ∼10 disaccharide transporter isoforms (Lalonde et al., 2004), and all of these plasma membrane–located carriers together with other homologous proteins from animals, fungi, and bacteria constitute a large protein family (Henderson, 1991; Saier, 2000).

In addition to transport across the plasma membrane, carrier-mediated sugar transport has also been demonstrated across organellar membranes such as the inner plastid envelopes (Schäfer et al., 1977; Rost et al., 1997) or the vacuolar tonoplast (Rausch, 1991; Martinoia et al., 2000). Vacuoles play a central role in the long-term or temporary storage of sugars. Storage tissues such as red beet (*Beta vulgaris*) and sugarcane (*Saccharum officinarum*) stalks accumulate large amounts of sucrose that is used as an energy source when these tissues turn to source metabolism (Buchanan et al., 2000). In leaves, sugars accumulate during the daytime and are released from the vacuole at night (Martinoia et al., 1987). In that case, the vacuole represents a short-time storage vessel that allows the plant to store excess soluble carbohydrates. Furthermore, several plants, such as barley (*Hordeum vulgare*) and wheat (*Triticum aestivum*), synthesize fructans in leaf vacuoles using sucrose as a precursor (Cairns et al., 2000).

Facilitated diffusion as well as energized proton antiport mechanisms have been described for monosaccharide and sucrose transport into isolated vacuoles or tonoplast vesicles prepared from a large number of plant species (Guy et al., 1979;

Thom and Komor, 1984; Daie and Wilusz, 1987; Martinoia et al., 1987; Rausch, 1991; Shiratake et al., 1997). Accordingly, putative tonoplast-localized sugar carriers have been identified in proteomic approaches (Carter et al., 2004; Endler et al., 2006) or in immunological studies (Chiou and Bush, 1996). It was recently shown that Hv Sut2 and At Suc4 transport sucrose (Weise et al., 2000; Weschke et al., 2000) and that these carriers reside in the vacuolar membrane (Endler et al., 2006). However, the exact role of these transport proteins is still open to debate. In chloroplasts, a glucose and a maltose transporter have been identified (Weber et al., 2000; Nittyla et al., 2004), but only the latter has been characterized on both the molecular and functional levels (Nittyla et al., 2004).

Here, we report on a monosaccharide transporter from *Arabidopsis*. This protein has three isoforms in *Arabidopsis*, and all members of this carrier group exhibit their highest sequence similarity to bacterial sugar carriers and not to the functionally analyzed plant plasma membrane–located hexose carriers (STP). Based on subcellular localization studies, on transport studies using isolated vacuoles from cold-adapted wild-type or knockout lines, and on altered sugar accumulation and allocation in knockout mutants during either cold adaptation or sugar feeding, we present evidence for vacuolar monosaccharide transporters from *Arabidopsis* at both the molecular and functional levels.

RESULTS

Amino Acid Sequence Analysis of *Arabidopsis* Tonoplast Monosaccharide Transporter–Type Proteins

During screening of the *Arabidopsis* EST library, we discovered a cDNA clone (No. 8B8T74) encoding a carrier exhibiting highest similarity to bacterial monosaccharide transporters. We sequenced the full-length clone and (after having performed localization studies; see below) named the deduced protein TONOPLAST MONOSACCHARIDE TRANSPORTER1 (TMT1). TMT1 comprises 734 amino acid residues and shows 32% similarity to the bacterial glucose transporter GTR from *Synechocystis* species and 26% similarity to the plasma membrane–located *Arabidopsis* glucose transporter STP1 (Figure 1). The substantially lower similarity of TMT1 to the sucrose transporter SUC1 (16%; Figure 1) further indicates that TMT1 is a member of the monosaccharide and not the disaccharide transporter family. Two additional TMT isoforms have been amplified via PCR from first-strand cDNA: TMT2 contains 739 amino acid residues, and TMT3 contains 729 amino acid residues (see Supplemental Figure 1 online). TMT proteins exhibiting substantial structural similarities to the *Arabidopsis* homologs have also been identified in dicotyledonous plants such as *Medicago* (accession number AC131026) and grape vine (*Vitis vinifera*; accession number AAX47312) and in monocotyledonous species such as barley (accession number Q8GT52) and rice (*Oryza sativa*; accession number Os02g13560). All members of the TMT protein group exhibit higher structural similarities to prokaryotic hexose carriers than to the plant plasma membrane–located and functionally analyzed carriers of the STP group (data not shown).

TMT1 exhibits 12 predicted transmembrane domains (Figure 1) and shows a uniquely large centrally located hydrophilic loop connecting transmembrane domains 6 and 7 (Figure 1). This loop spans ~320 amino acid residues in length, which is nearly four to five times larger than the corresponding structures in all other known monosaccharide transporters from prokaryotes and eukaryotes, and is not present in the *Synechocystis* homolog (Henderson, 1991; Mueckler, 1993; Barrett et al., 1999). Similar to TMT1, isoforms TMT2 and TMT3 also exhibit an extraordinary long centrally located loop (see Supplemental Figure 1 online).

Subcellular Localization of *Arabidopsis* TMT Proteins

Recently, a proteome analysis of the *Arabidopsis* and barley tonoplast indicated the presence of TMT1 and TMT2 in this membrane (Carter et al., 2004). However, because proteome analyses might provide false information on the presence of proteins in specific subcellular fractions as a result of contamination from other organelles, we used an alternative approach by expressing TMT–green fluorescent protein (GFP) fusion proteins in both tobacco (*Nicotiana tabacum*) protoplasts and *Arabidopsis* cell suspension culture protoplasts. We included TMT3 in this analysis because, in contrast with TMT1 and TMT2, the third TMT isoform has not been identified in a proteome analysis (Carter et al., 2004).

Figure 2A shows chlorophyll autofluorescence in chloroplasts present in an isolated tobacco protoplast. TMT1-GFP fluorescence is clearly distinct from chloroplast autofluorescence and reveals a tonoplast and not a plasma membrane localization of the fusion protein. This tonoplast localization is indicated because of the large size of the marked membrane, which appears sporadically indented by chloroplasts (Figure 2B), and is further substantiated in the merged image (Figure 2C). Similarly, the transient expression of *TMT1-GFP* in protoplasts from an *Arabidopsis* suspension culture leads to decoration of the tonoplast (Figure 2E). The corresponding merged image (Figure 2F) clearly revealed the thin cytoplasmic space between the labeled tonoplast and the plasma membrane.

As shown for TMT1-GFP, the fusion protein TMT3-GFP is also located in the vacuolar membrane from both transiently transformed *Arabidopsis* suspension culture cells and tobacco protoplasts (data not shown; see Supplemental Figures 2A to 2C online).

Tissue, Cell, and Stress Specificity of *TMT1, TMT2,* and *TMT3* Gene Expression

RNA gel blot hybridization analysis revealed the highest *TMT1* mRNA levels in juvenile (sink) and adult (source) leaves, followed by flower tissues (Figure 3). Root and stem tissues accumulated substantially less *TMT1* transcript (Figure 3). By contrast, *TMT2* mRNA accumulated mainly in root and stem tissues and less in juvenile and adult leaves or in flower tissues (Figure 3). Interestingly, *TMT3* mRNA was not detectable by RNA gel blot analysis (data not shown), indicating a very low expression level.

To gain more information on the promoter activity of all three *TMT* genes, we generated *TMT1-*, *TMT2-*, and *TMT3-promoter*–β-glucuronidase (GUS) plants. Figure 4A reveals that the *TMT1* gene is actively transcribed in pollen cells and in all tissues from developing seedlings at 2 d after germination. Young leaves from
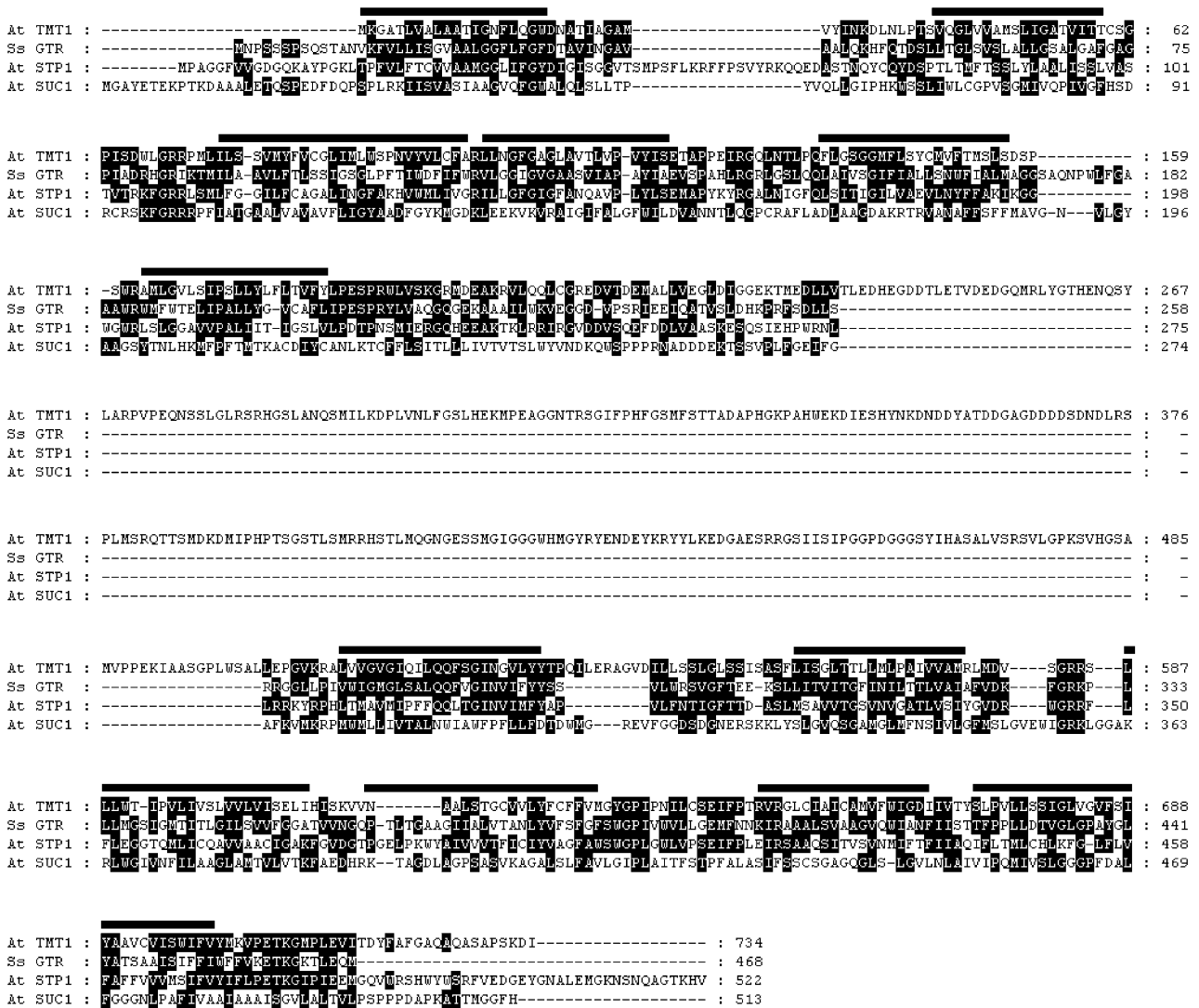
Figure 1. Alignment of the Amino Acid Sequences of TMT1 and Selected Sugar Transporters.

At, *Arabidopsis thaliana*; GTR, glucose transporter; Ss, *Synechocystis* species PCC6803; STP1, plasma membrane–located sugar (monosaccharide) transporter; SUC1, plasma membrane–bound sucrose transporter; TMT1, TONOPLAST MONOSACCHARIDE TRANSPORTER1. Numbers indicate amino acid positions, and black bars indicate transmembrane domains of TMT1 predicted by the program SOAP in PCgene.

plants grown on soil (3 weeks old) exhibited slightly higher *TMT1-promoter*–GUS activity than older leaves (Figure 4A). *TMT1* expression in flowers is attributable mainly to its expression in petals, filaments, and pollen cells still wrapped by anther envelopes (Figure 4A). Developing seeds, still embedded in siliques, did not exhibit substantial GUS activity (Figure 4A). Thin cuts of embedded leaves showed that *TMT1* is expressed in different cell types. *TMT1* gene expression is most prominent in mesophyll cells and in cells surrounding the vascular tissue and lower epidermis and is less prominent in the upper epidermis (see Supplemental Figure 3 online).

Figure 4B shows that *TMT2-promoter*–GUS activity is relatively low in germinating seedlings (at day 2 after germination) or in 5-d-old cotyledons. In young roots, *TMT2-promoter*–GUS activity was restricted to the stele, and in mature leaves, only the edge areas showed GUS activity (Figure 4B). In undeveloped floral side buds, in petals, and in filaments, *TMT2-promoter*–GUS activity was substantial.

TMT3 mRNA was not detectable by RNA gel blot analysis (see above). Accordingly, *TMT3-promoter*–GUS activity was low in all tissues tested. *Arabidopsis* tissues manifesting *TMT1-* and/or *TMT2-promoter*–GUS activity, such as young leaves and filaments, did not exhibit *TMT3-promoter*–GUS activity (Figure 4C). Only at the very edges of source leaves was a limited *TMT3-promoter*–GUS activity present. In sum, we found that *TMT3-promoter*–GUS activity was low in all tissues tested and that *TMT1-* and *TMT2-promoter*–GUS activities differed in tissue specificity and developmental stage.
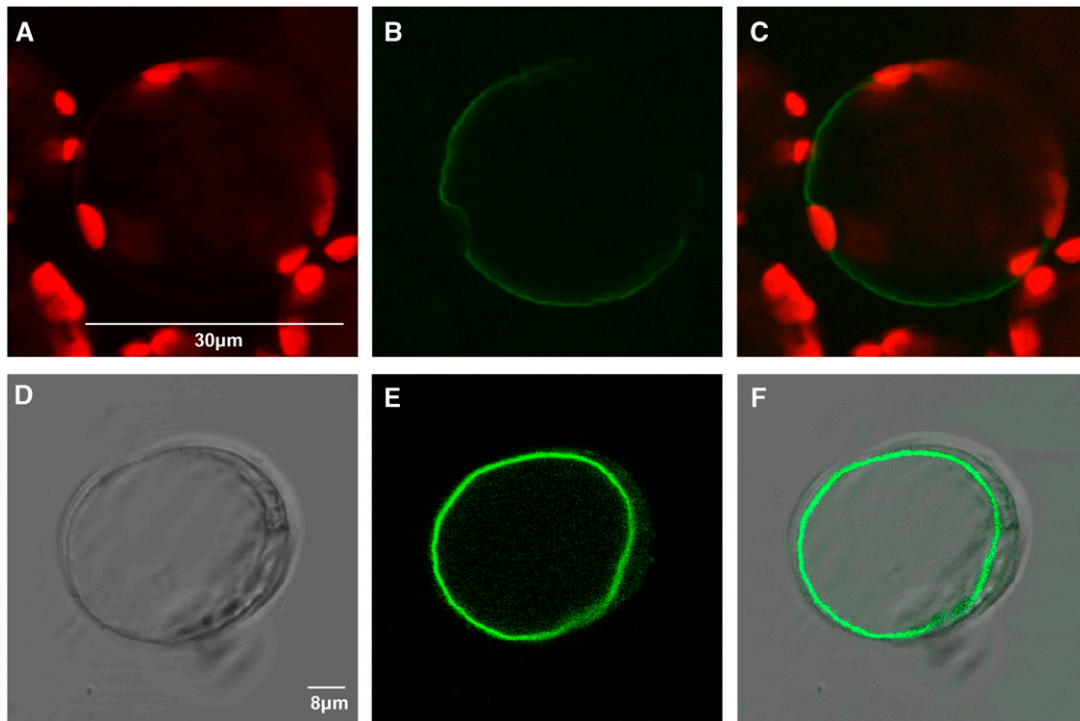
Figure 2. Subcellular Localization of an N-Terminal TMT1-GFP Fusion Protein in Tobacco Protoplasts or Protoplasts from an *Arabidopsis* Suspension Culture.

(A) Autofluorescence of chloroplasts in tobacco protoplasts.
(B) Localization of the TMT1-GFP fusion protein in tobacco protoplasts.
(C) Merge of **(A)** and **(B)**.
(D) Bright-field image of an *Arabidopsis* cell suspension protoplast.
(E) Localization of the TMT1-GFP fusion protein in an *Arabidopsis* suspension culture cell.
(F) Merge of **(D)** and **(E)**.

To obtain information on how different environmental or stress conditions act on *TMT* gene expression, we analyzed alterations of corresponding mRNA levels in response to cold treatment, to sugar or salt level, and to drought. Already after 24 h in the cold (9°C), mature *Arabidopsis* plants had increased *TMT1* mRNA content, and after 48 h in the cold, *TMT1* mRNA reached a maximal level that did not increase further (Figure 5). *TMT2* mRNA levels did not respond markedly to cold treatment, as there was only a slight increase of *TMT2* mRNA after 24 h in the cold compared with the level at the beginning of the experiment (Figure 5). Control plants (kept at standard growth conditions, 21°C) showed exactly the same *TMT1* and *TMT2* mRNA levels as at the beginning of the experiment, and cold treatment did not promote the accumulation of *TMT3* mRNA above the detection level (data not shown).

The presence of high sugar levels during the growth of *Arabidopsis* in liquid culture medium (Scheible et al., 2004) also affected *TMT1* and *TMT2* mRNA levels (Figure 5). The addition of 5% glucose promoted the accumulation of both *TMT1* and *TMT2* mRNA (Figure 5). Five percent fructose in the growth medium slightly stimulated *TMT2* but not *TMT1* mRNA accumulation, and the presence of sucrose (1 or 5%) led to a higher accumulation of *TMT1* mRNA compared with *TMT2* mRNA (Figure 5). Similar to cold treatment, the presence of sugars did not promote the

accumulation of *TMT3* mRNA above the detection level (data not shown).

When *Arabidopsis* plants were subjected to salt stress by increasing NaCl concentrations in the growth medium, accumulation of *TMT1* and *TMT2* mRNA was observed (Figure 5). However,
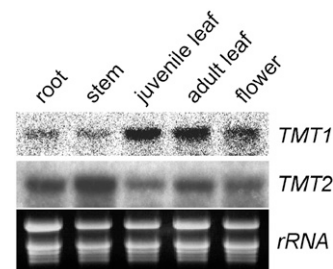

Figure 3. RNA Gel Blot Analysis of *TMT1* and *TMT2* Transcript Accumulation in Various *Arabidopsis* Tissues.

Plants were grown for 6 to 14 weeks under standard growth conditions. Flower and stem tissues were taken from ∼12- to 14-week-old plants. Full length cDNAs of *TMT1* and *TMT2* were used as probes. The high specificity of probes used was analyzed by dot blot (data not shown).
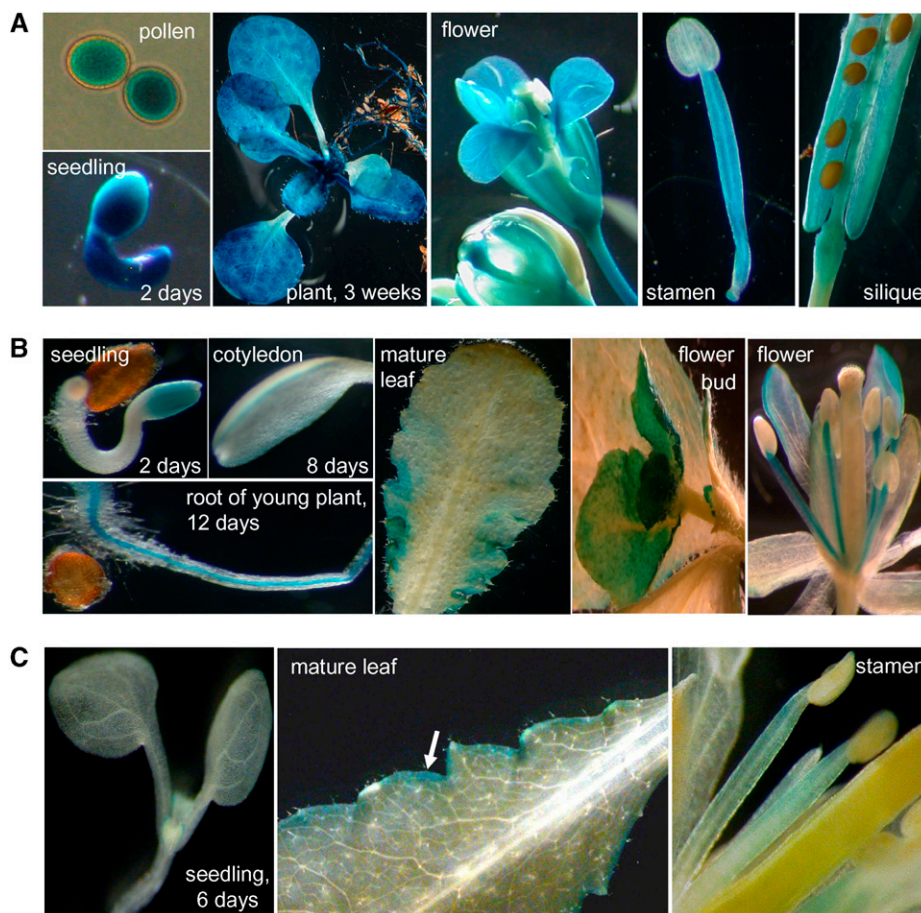
Figure 4. Histochemical Localization of *TMT* Gene Expression.

(A) *TMT1-promoter*–GUS.
(B) *TMT2-promoter*–GUS.
(C) *TMT3-promoter*–GUS.

the salt concentrations required to attain the highest *TMT1* and *TMT2* transcripts were different: 150 mM NaCl provoked the highest *TMT1* mRNA levels, whereas *TMT2* mRNA levels attained their maximum at 200 mM NaCl (Figure 5). NaCl did not promote the accumulation of *TMT3* mRNA (data not shown).

Drought stress, induced by stopping watering of soil-grown *Arabidopsis* plants, stimulated the accumulation of *TMT1* mRNA (Figure 5). Seven days after stopping watering, *TMT1* transcripts were significantly higher than at the beginning of the experiment or in daily-watered control plants (Figure 5; data not shown). After 7 d of drought treatment, *TMT2* mRNA accumulated slightly (Figure 5), but drought stress did not promote any detectable accumulation of *TMT3* mRNA (data not shown).

Identification of *tmt* Knockout Mutants

Knockout mutants created by T-DNA insertions represent a frequently used powerful system to study the physiological function of a protein. A T-DNA insertion mutant for TMT1 has been identified in the Syngenta library and has been named

tmt1::tDNA1. The T-DNA insertion in this mutant is located in exon 1 (Figure 6A). The homozygous genotype of the *tmt1::tDNA1* mutation has been confirmed by PCR on genomic DNA (see Supplemental Figure 4A online). RT-PCR analysis showed the absence of *tmt1* mRNA in the mutant plant (Figure 6B). Similarly, *tmt1::tDNA2* contains a T-DNA insertion in exon 3 (Figure 6A). The homozygous genotype of the *tmt1::tDNA2* mutation has been confirmed by PCR on genomic DNA (see Supplemental Figure 4A online). RT-PCR analysis showed the absence of *tmt1* mRNA in the mutant (Figure 6B).

The *tmt2::tDNA* line contains a T-DNA insertion in exon 5 (Figure 6A). The homozygous genotype of the *tmt2::tDNA* mutation was confirmed by PCR on genomic DNA (see Supplemental Figure 4B online), and RT-PCR analysis revealed the absence of *tmt2* mRNA in the mutant (Figure 6B). Finally, the *tmt3::tDNA* contains a T-DNA insertion in exon 3 (Figure 6A). The homozygous genotype of the *tmt3::tDNA* mutation was confirmed by PCR on genomic DNA (see Supplemental Figure 4B online), and RT-PCR analysis confirmed the absence of *TMT3* mRNA in the mutant (Figure 6B).
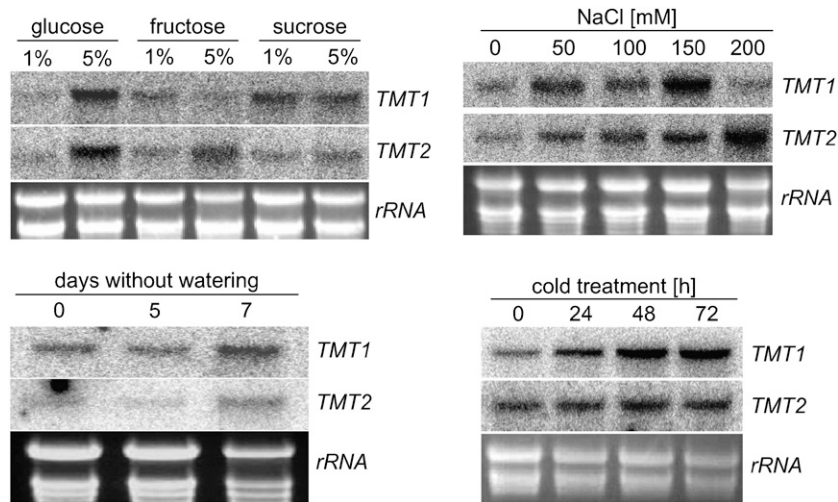
Figure 5. RNA Gel Blot Analysis of *TMT1* and *TMT2* mRNA Accumulation in Response to Sugar Availability and Environmental Stress Stimuli.

For analysis of the effects of salt treatment on gene expression, total RNA of 7-d-old seedlings grown on Murashige and Skoog (MS) agar medium was harvested. For analysis of the effects of sugar feeding on gene expression, total RNA of 7-d-old seedlings grown in liquid culture was harvested. Five percent monosaccharide represents a concentration of ~280 mM, and 5% sucrose represents a concentration of ~146 mM. For analysis of the effects of cold and drought stress on gene expression, total RNA of leaves from 5-week-old soil-grown plants was isolated. Total RNA represents the loading control.

In addition to these single knockout lines, we also created double and triple *tmt* knockout mutants by crossing the single knockout plants. A double knockout line was created by crossing *tmt1::tDNA1* with *tmt2::tDNA* (see Supplemental Figure 4C online). RT-PCR analysis showed the absence of *tmt1* and *tmt2* mRNA in the double mutant (Figure 6B). For generation of a triple mutant, we crossed the homozygous double mutant with the homozygous *tmt3::tDNA* line and identified the corresponding mutant lacking all functional *TMT* genes (see Supplemental Figure 4D online). RT-PCR analysis confirmed the absence of all three *TMT* mRNA species in the triple mutant (Figure 6B). None of the mutants mentioned exhibited any distinctive phenotypic features when grown under standard growth conditions.

Monosaccharide Transport into Isolated Vacuoles from Wild-Type Plants or *tmt* Knockout Mutants

To this point, it was impossible to detect glucose transport activity by heterologous expression of any of the three TMT proteins in bakers' or fission yeast mutants lacking endogenous glucose carriers, or in *Pichia pastoris* (data not shown). This result is in agreement with the failure of another research group trying to express the sugarcane homolog (Casu et al., 2003). Although the yeast lines mentioned above exhibited large amounts of *TMT1*, *TMT2*, or *TMT3* mRNA (data not shown), the corresponding TMT proteins were always absent, as revealed using either a His tag–specific antibody or an antibody raised against the large hydrophilic loop present in TMT1 (Figure 1; data not shown).

However, we have shown that the *TMT1* gene in particular is strongly induced during cold adaptation and is highly responsive upon glucose administration (Figure 5). Therefore, it was of interest to analyze whether monosaccharide transport into the *Arabidopsis* vacuole is increased after cold adaptation. For this purpose, we isolated leaf mesophyll vacuoles either from control wild-type plants (grown under standard growth conditions at 21°C) or from plants transferred for 2 d into the cold (9°C) before vacuole isolation.

Wild-type vacuoles isolated from plants grown under standard growth conditions took up 0.28 nmol [^{14}C]glucose/μL vacuole after 10 min of incubation, whereas vacuoles isolated from wild-type plants previously incubated for 2 d at 9°C exhibited an internal concentration of 0.83 nmol [^{14}C]glucose/μL vacuole after 10 min of incubation (Figure 7A).

To gain further insight into the biochemical characteristics of TMT-catalyzed sugar import, we analyzed the effect of ammonium, fructose, or the sugar transporter inhibitor phlorizin on glucose import into wild-type vacuoles (Figure 7B). The presence of the protonophore NH$_4$Cl (5 mM) reduced the glucose import rate into isolated vacuoles from cold-induced *Arabidopsis* plants by ~42%, 5 mM fructose inhibited glucose uptake by ~45%, and 1 mM phlorizin reduced glucose uptake by ~81% (Figure 7B). Higher phlorizin concentrations did not result in any further reduction in glucose uptake (data not shown).

To determine whether the T-DNA insertion in the *TMT1* gene correlates with decreased glucose uptake activity into corresponding vacuoles, we compared glucose uptake rates into vacuoles isolated from wild-type, *tmt1::tDNA1*, and *tmt1::tDNA2* plants. For this experiment, all plant lines were transferred for 2 d into the cold (9°C) before vacuole isolation. After 10 min of incubation, wild-type vacuoles contained 0.92 nmol [^{14}C]glucose/μL vacuole, whereas *tmt1::tDNA1* and *tmt1::tDNA2* vacuoles had taken up 0.34 and 0.39 nmol [^{14}C]glucose/μL vacuole, respectively, within the same time (Figure 7C). This result reveals
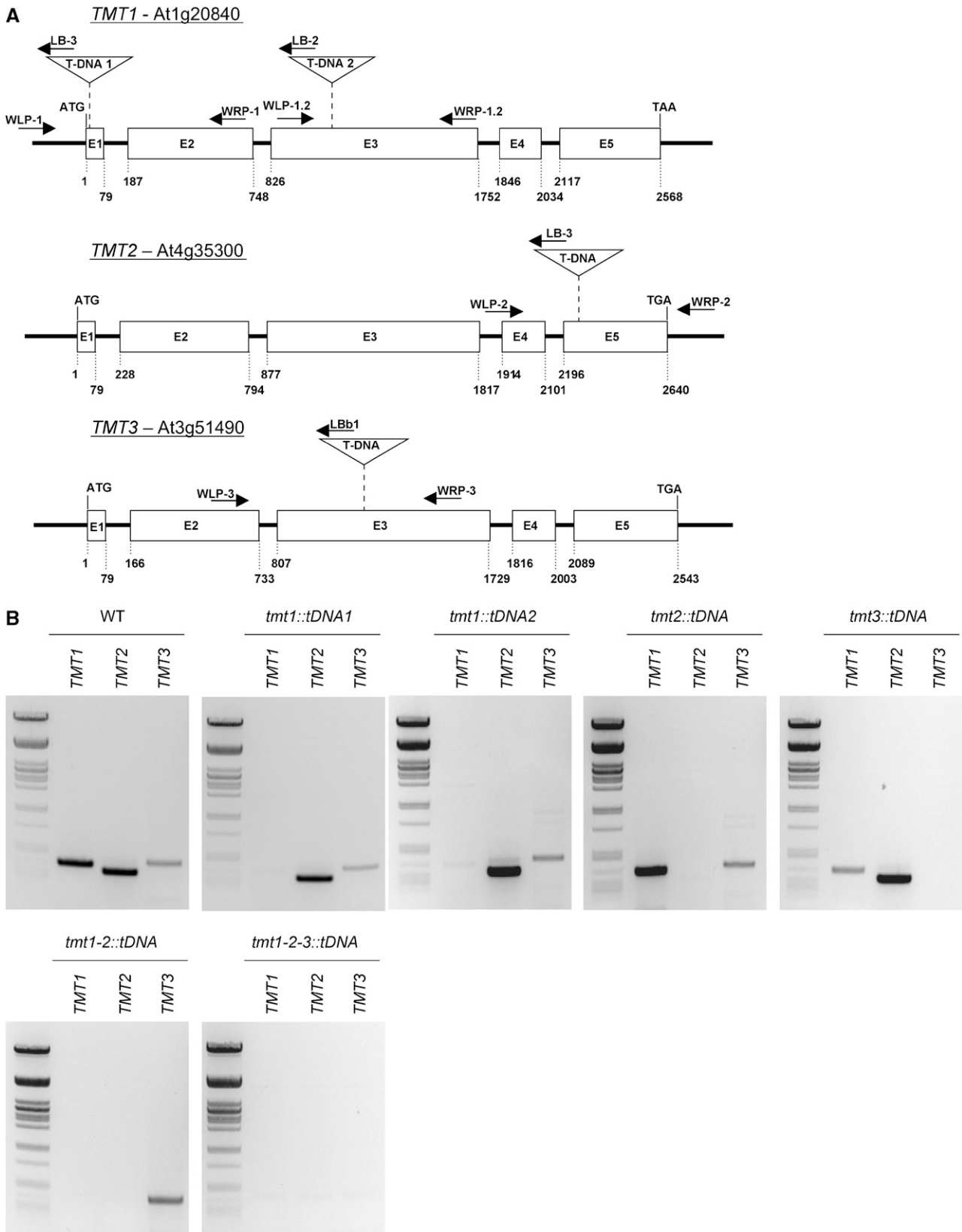
Figure 6. Molecular Characterization of Homozygous *tmt1::tDNA1*, *tmt1::tDNA2*, *tmt2::tDNA*, and *tmt1-2-3::tDNA* Mutants.

that the two independent *tmt1* knockout lines exhibited a substantially reduced capacity to import glucose into the vacuole.

Although homolog 1 was the most prominently expressed *TMT* gene in *Arabidopsis* leaves (Figures 3 and 4A), it was of interest to reveal whether glucose transport into vacuoles isolated from the triple *tmt* knockout line was decreased further. Therefore, we isolated vacuoles from cold–induced wild-type and *tmt* triple mutant plants and compared the relative glucose uptakes. From Figure 7D, it is obvious that glucose uptake into triple knockout vacuoles was significantly lower than into wild-type vacuoles. However, the decrease observed in the triple mutant was not substantially lower than that observed in the two independent *tmt1::tDNA* knockout lines (Figures 7C and 7D).

Sugar Levels in Wild-Type Plants and *tmt* Knockout Mutants

Under standard growth conditions (10 h of light, 21°C), none of the TMT mutants (including the triple mutant) showed any visible phenotypic difference compared with wild-type plants. However, because *TMT1* and *TMT2* are induced in the cold and because vacuolar glucose transport activity is strongly upregulated during cold incubation, we were interested to know whether this observation is also reflected by the leaf sugar content in the chosen growth conditions.

Under standard growth conditions, glucose contents were 0.57 μmol/g fresh weight in wild-type plants and 0.39 and 0.41 μmol/g fresh weight, respectively, in the two *tmt1* mutant lines (Figure 8A), representing slightly (~30%) reduced glucose contents. A similar reduction (~28%) was also observed for fructose (Figure 8A), whereas sucrose contents were very similar in wild-type and mutant plants (Figure 8A). *tmt2::tDNA* and *tmt3::tDNA* lines grown under standard growth conditions did not exhibit any altered sugar levels compared with wild-type plants (data not shown). The double knockout plant and the triple knockout line showed similarly reduced glucose and fructose levels as the *tmt1* T-DNA lines when grown under standard conditions, whereas the triple mutant contained less glucose and fructose. Glucose amounted to 0.45 and 0.24 μmol/g fresh weight in the double and triple mutants, respectively, and fructose accumulated to 0.11 and 0.05 μmol/g fresh weight in the double and triple mutants, respectively (Figure 8A).

To analyze whether the differences observed for glucose and fructose would be more pronounced during cold stress (leading to the accumulation of *tmt1* and *tmt2* mRNA; Figure 5), we transferred wild-type and knockout plants into the cold (9°C) and incubated the plants for 24 h under permanent light (light was given to promote net sugar accumulation by photosynthesis). Twenty-four hours after transfer of wild-type plants into the cold,

glucose accumulated ~10-fold to a concentration of 5.5 μmol/g fresh weight, fructose accumulated to 2.3 μmol/g fresh weight, and sucrose doubled to ~2.4 μmol/g fresh weight (Figure 8B). However, in both knockout lines, the changes in monosaccharides differed markedly from the corresponding changes in wild-type leaves. Twenty-four hours after transfer into the cold, *tmt1::tDNA1* and *tmt1::tDNA2* leaves contained only 2.0 and 2.7 μmol glucose/g fresh weight, respectively (Figure 8B). Fructose accumulated in both knockout lines to only 0.5 and 0.7 μmol/g fresh weight, respectively (Figure 8B). Interestingly, under cold stress conditions, the double *tmt* mutant contained significantly less hexose compared with the single *tmt1* T-DNA insertion lines (0.52 μmol/g fresh weight glucose and 0.14 μmol/g fresh weight fructose) (Figure 8B). Upon cold stress, the triple mutant contained glucose and fructose levels similar to concentrations observed in the double mutant, namely 0.53 μmol/g fresh weight glucose and 0.12 μmol/g fresh weight fructose. In contrast with the two *tmt1* knockout mutants, the double and triple mutants also showed slightly reduced sucrose levels upon 24 h of cold stress (Figure 8B).

Sugar Feeding into Leaf Discs from Wild-Type or *tmt1::tDNA* Lines

An impaired glucose transport into the vacuole may lead to increased cytosolic glucose concentrations and thus affect carbohydrate-regulated genes. The *CHLOROPHYLL$_{ab}$ BINDING PROTEIN1* gene (*CAB*) and *NITRATE REDUCTASE1* (*NR1*) represent sugar-regulated plant genes (Koch, 1996). Therefore, these two genes are suitable candidates to test whether cytosolic glucose contents are altered in TMT1 mutants, because if this is the case, altered transcript levels should be observed. For this analysis, leaf discs from 4- to 5-week-old plants were prepared 3 h after the onset of illumination and subsequently incubated for 24 h in the dark in the presence of various sugars (each sugar was present at a concentration of 100 mM). Dark incubation was chosen to prevent photosynthesis-driven sugar accumulation. Subsequently, total RNA from leaf discs was isolated and RNA gel blot hybridization was conducted to quantify the levels of *CAB* mRNA (known to be downregulated by sugars) and *NR1* mRNA (known to be upregulated by sugars) (Koch, 1996).

At the beginning of the incubation experiment, leaves from wild-type and the two independent knockout plants contained very similar levels of *CAB* and *NR1* mRNA, respectively (Figure 9). Wild-type leaf discs incubated in the presence of glucose, fructose, or sorbitol showed no obvious decrease of *CAB* mRNA compared with the 0-h control, whereas sucrose provoked a

---

Figure 6. (continued).

(A) Positions of T-DNA insertions in the *TMT* genes. Arrows indicate primer positions and the direction of polymerase activity. Primer sequences are given in the legend to Supplemental Figure 4 online.

(B) RT-PCR analysis of cDNA extracted from leaves of wild-type, *tmt1::tDNA1*, *tmt1::tDNA2*, *tmt2::tDNA*, *tmt1-2::tDNA*, and *tmt1-2-3::tDNA* plants with gene-specific primer pairs. To reveal the presence of *TMT1* mRNA, the primer pair AW31 and AW32 was used; to reveal the presence of *TMT2* mRNA, the primer pair AW29 and AW30 was used; and to reveal the presence of *TMT3* mRNA, the primer pair AW27 and AW28 was used. The size standard used is a *Pst*I-digested λ-phage DNA.
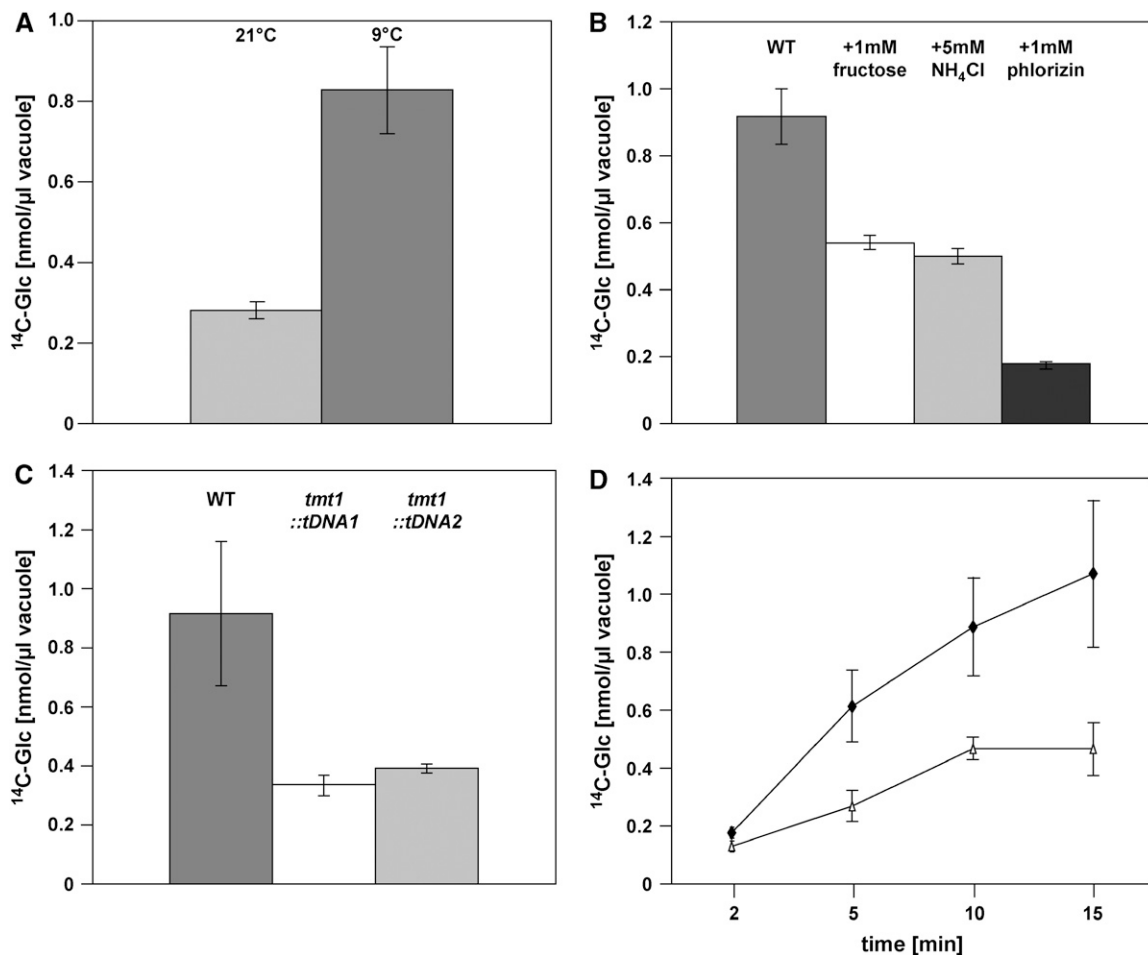
Figure 7. Uptake of [^{14}C]Glucose into Isolated *Arabidopsis* Mesophyll Vacuoles.

(A) Effects of cold treatment on glucose uptake into wild-type vacuoles. Plants were either grown under standard growth conditions or incubated for 2 d at 9°C before vacuole isolation. Transport of [U-^{14}C]glucose (100 μM) was conducted for 10 min.

(B) Effector studies of glucose uptake into vacuoles isolated from cold-induced wild-type plants. Plants were incubated for 2 d at 9°C before vacuole isolation. Labeled glucose was given at a concentration of 100 μM. Effectors were given at the indicated concentrations. [U-^{14}C]glucose (100 μM) uptake was allowed for 10 min.

(C) Glucose uptake into vacuoles isolated from wild-type, *tmt1::tDNA1-*, and *tmt1::tDNA2* plants. Plants were incubated for 2 d at 9°C before vacuole isolation, and labeled glucose was given at a concentration of 100 μM.

(D) Time course of glucose uptake into vacuoles isolated from wild-type and *tmt1-2-3::tDNA* plants. Plants were incubated for 2 d at 9°C before vacuole isolation, and radioactively labeled glucose was given at a concentration of 100 μM. Open triangles represent vacuoles from *tmt1-2-3::tDNA* plants, and closed diamonds represent vacuoles from wild-type plants.

All data given represent means of three individual experiments, each with three to four replicate samples, ± SE.

decrease of *CAB* mRNA (Figure 9). Interestingly, in both TMT1 knockout lines, the sugars glucose, fructose, and sucrose induced a significantly stronger decrease of *CAB* mRNA compared with the corresponding wild-type leaf discs (Figure 9).

The levels of *NR1* mRNA in wild-type leaf discs incubated in sugars were higher than those in leaf discs incubated in water (Figure 9). This observation concurs with the known sugar induction of the *NR1* gene (Koch, 1996). However, each of the sugars tested provoked a stronger stimulatory effect upon the *NR1* gene in leaf discs prepared from *tmt1::tDNA1* or *tmt1::tDNA2* plants (Figure 9).

DISCUSSION

Sugars fulfill many essential functions in all types of plant cells. Therefore, it is not surprising that lower and higher plant species possess a large number of sugar transporter isoforms exhibiting tightly controlled cell- and tissue-specific expression patterns (Büttner and Sauer, 2000). Here, we describe a monosaccharide carrier, named TMT, that has three isoforms in *Arabidopsis* (Figure 1; see Supplemental Figure 1 online). The occurrence of TMT-type sugar carriers is not restricted to *Arabidopsis*, as a homolog has been identified in sugarcane (Casu et al., 2003).
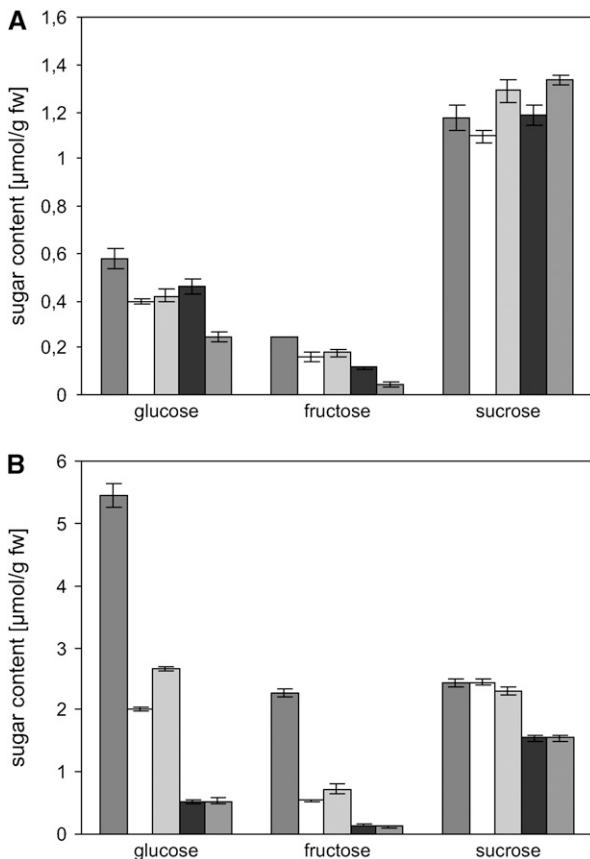
Figure 8. Effects of Cold Treatment on Sugar Levels in *Arabidopsis* Leaves.

(A) Sugar contents in leaves from 5-week-old wild-type, *tmt1::tDNA1*, *tmt1::tDNA2*, *tmt1-2::tDNA*, and *tmt1-2-3::tDNA* plants.

(B) Sugar levels from 5-week-old wild-type, *tmt1::tDNA1*, *tmt1::tDNA2*, *tmt1-2::tDNA*, and *tmt1-2-3::tDNA* plants after 24 h of cold stress (9°C) and permanent light. Dark gray bars represent wild-type samples, white bars represent *tmt1::tDNA1* samples, light gray bars represent *tmt1::tDNA2* samples, black bars represent *tmt1-2::tDNA* samples, and middle gray bars represent *tmt1-2-3::tDNA* samples.

Data represent means of three independent experiments ± SE.

Although the transport activity and the subcellular localization of the sugarcane carrier have not been demonstrated, it has been speculated that this transport protein might be involved in cellular sugar import (Casu et al., 2003). By contrast, we present evidence that TMT proteins from *Arabidopsis* reside in the tonoplast, as suggested from vacuolar proteome data (Carter et al., 2004; Endler et al., 2006), and that these transporters play a central role in vacuolar hexose transport, mainly under stress conditions.

The structural similarities between TMT proteins and the cyanobacterial monosaccharide transporter GTR (Figure 1; see Supplemental Figure 1 online) appear remarkable considering the long evolutionary distance between plants and prokaryotes. However, because of the presence of TMT homologs in two cyanobacterial species, namely *Synechocystis* species (Figure 1)

and *Nostoc punctiforme* (data not shown), it is possible to develop an evolutionary scenario explaining the presence of these transporters in plants. Accordingly, this gene was integrated into the nuclear genome during early plant evolution, but the gene product was not recruited to the inner plastidic envelope membrane but to the tonoplast (Figure 2; see Supplemental Figure 2 online) (Carter et al., 2004). The localization of TMT1 in a cell compartment different from the plastid is consistent with the absence of an N-terminal transit peptide in all TMT proteins (see Supplemental Figure 1 online) required for the integration of membrane proteins into the inner plastidic envelope membrane (Flügge, 1999).

In contrast with all other plant monosaccharide transporters analyzed to date at the functional level (Büttner and Sauer, 2000), TMT proteins reside in the vacuolar membrane. Here, we present two observations strongly indicating a vacuolar localization of TMT proteins: first, TMT1- and TMT3-GFP proteins transiently synthesized in tobacco protoplasts or in *Arabidopsis* suspension culture cells reside in the tonoplast (Figure 2; see Supplemental Figure 2 online); second, vacuoles isolated from two independent *tmt1::tDNA* mutant lines, or from the *tmt* triple mutant, exhibited substantially reduced rates of glucose import (Figures 7C and 7D). Moreover, two of the three TMT proteins have been identified in the tonoplast within a proteomic analysis (Carter et al., 2004). In addition, the observation that glucose and fructose accumulation is impaired in the cold further indicates that TMT proteins reside in the tonoplast and contribute to monosaccharide transport.

It is well known that in *Arabidopsis* leaves, osmotic or cold stress leads to the degradation of starch and consequently to increased glucose levels (Alberdi and Corcuera, 1991; Yano et al., 2005; Kaplan et al., 2006). Interestingly, both of these environmental stimuli induced the accumulation of *tmt1* mRNA (Figure 5), and concomitantly, a strong stimulation of glucose uptake into isolated mesophyll vacuoles was observed in wild-type plants (Figure 7A). This correlation leads to the conclusion
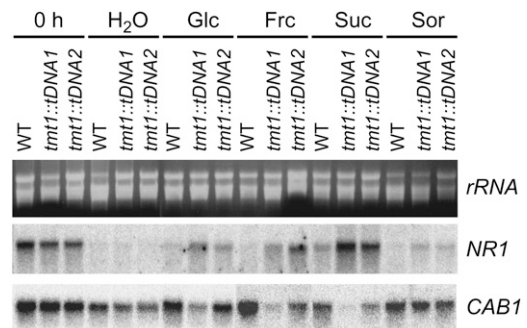

Figure 9. Quantification of mRNA Coding for *CAB1* or *NR1* in Leaf Samples from Wild-Type, *tmt1::tDNA1*, and *tmt1::tDNA2* Plants.

Leaf discs were taken from 6-week-old soil-grown plants at 3 h after illumination and incubated for 24 h in the dark in either water or water supplemented with the solutes indicated (each at 100 mM). Subsequently, total RNA was isolated and probed for the relative abundance of mRNA coding for *CAB1* or *NR1*. rRNA represents the loading control. Sor, sorbitol.

that TMT1 transport is regulated at the transcriptional level. However, we cannot exclude the possibility that posttranslational modification of TMT1 or the two additional isoforms occurs and contributes to an upregulation of vacuolar glucose import upon cold induction. Nevertheless, because vacuoles from *tmt* knockout plants exhibit a far lower glucose transport activity (Figures 7C and 7D) and because *tmt* mutants are substantially impaired in cold-induced accumulation of monosaccharides (Figure 8B), these carriers are likely to be central elements of vacuolar glucose and fructose accumulation during the cold stress response.

The observation that both the *TMT1* and *TMT2* genes are induced by sugar feeding (Figure 5) might additionally be taken as further indication for an in vivo transport function of TMT proteins. Keeping in mind that the vacuole contains the largest part of monosaccharides in mesophyll cells (Farré et al., 2001), sugar feeding induces carbohydrate accumulation in the cytoplasm and the subsequent accumulation in the vacuole. However, sugar sensing takes place in the cytosol by specific hexokinases (Jang et al., 1997), and both *tmt1* knockout lines exhibited an oversensitized molecular sugar response, as revealed by the strong repression of *CAB1* mRNA and the increased accumulation of *NR1* mRNA compared with wild-type plants (Figure 9). This oversensitized sugar response strongly suggests that *tmt* knockout mutants cannot transfer freshly imported sugars into the vacuole as efficiently as the wild-type plants. In this way, sugars accumulate in the cytosol, where they induce a signal cascade leading to the deregulation of *CAB1* and *NR1* gene expression (Figure 9). This observation proves the importance of the efficient transfer and temporary deposition of metabolites for an optimal regulation of cytosolic carbohydrate metabolism.

The TMT protein family comprises three isoforms in *Arabidopsis* (see Supplemental Figure 1 online). According to the gene expression analysis (Figure 3) and *promoter*–GUS activity studies (Figure 4A), *TMT1* is the most highly expressed member of this family in *Arabidopsis* leaves. These data are in accordance with those from the GENEVESTIGATOR database (Zimmermann et al., 2004), in which the maximal expression level of *TMT1* in leaves is ∼3-fold that of *TMT2* and at least 10-fold that of *TMT3*. Interestingly, *TMT1* gene expression, and partly *TMT2* gene expression, is strong in young developing tissues and in pollen cells (Figure 4). Cells in young tissues and pollen cells are characterized by a rapid expansion, and it is possible that monosaccharide transport catalyzed by TMT proteins contributes to some extent to this process.

The *tmt1* knockout mutants exhibit ∼60% reduced glucose transport activity compared with wild-type plants (Figure 7C). This reduction is not increased further in the triple deletion mutant. (Figures 7C and 7D). However, the results on sugar accumulation during cold stress indicate that TMT2 (which is also induced under these conditions) might also play a role in the vacuolar hexose allocation in leaves. During cold stress, the *tmt1-2::tDNA* double mutant accumulates consistently less glucose and fructose than the *tmt1* single knockout lines (Figure 8B). The discrepancy between the transport results and the sugar accumulation pattern could be attributable to different causes. (1) Vacuole uptake experiments on *Arabidopsis* vacuoles are extremely difficult to carry out and always exhibit a considerable

standard deviation. Therefore, small differences observed between *tmt1* and *tmt1-2* knockout lines will not be statistically significant. (2) According to a recent gene expression analysis, *TMT1* mRNA is distributed similarly between mesophyll and epidermis cells, whereas *TMT2* mRNA is preferentially present in the epidermis (Suh et al., 2005). However, the vacuole isolation procedure established by us selects for mesophyll vacuoles, whereas sugar quantifications were performed on whole leaf extracts. However, in whole leaf extracts, the role of TMT2 might be more visible, because the corresponding gene appears to be highly expressed in the epidermis layers. (3) Vacuole transport studies were performed at a relatively low substrate concentration (100 µM). However, it cannot be excluded that TMT1 and TMT2 exhibit different kinetic properties and that TMT2 possesses a lower affinity for glucose and hence plays a minor role at the concentration tested. To perform a careful biochemical analysis of TMT1, TMT2, and TMT3, either a non-yeast-based expression system has to be established that allows the synthesis of these intracellular monosaccharide transporters or, alternatively, overexpression and purification of the TMT proteins in planta and subsequent incorporation in liposomes have to be envisaged.

Phlorizin, a known inhibitor of a wide range of monosaccharide carriers (Ehrenkranz et al., 2005), inhibited glucose import into isolated vacuoles below the level of glucose import present in vacuoles isolated from the *tmt* triple mutant (Figure 7). This observation indicates that besides the contribution of TMT1, TMT2, and TMT3 to vacuolar glucose import, other tonoplast-localized monosaccharide transporters exist. In any case, the biochemical data from isolated wild-type vacuoles reveal that the TMT1-coupled glucose transport is inhibited by the protonophore NH_4^+ and by fructose (Figure 7B). The inhibitory effect of NH_4^+ (Figure 7B) substantiates the assumption that glucose import linked to the presence of TMT1 is energy-dependent. This conclusion is in agreement with the observation that a fraction of the total vacuolar glucose transport capacity is dependent upon an existing proton motive force (Rausch, 1991; Martinoia and Ratajczak, 1997).

The observation that *tmt* knockout lines showed a markedly reduced ability to accumulate glucose and fructose upon cold stress (Figure 8B) can be taken as indirect evidence that TMT proteins accept both monosaccharides as substrates. However, the inhibitory effect of fructose on glucose uptake into cold stress–induced *Arabidopsis* vacuoles (Figure 7B) provides further experimental evidence that TMT proteins accept both sugars as substrates. This conclusion is in agreement with the biochemical properties of the cyanobacterial homolog GTR (Schmetterer, 1990).

Interestingly, a proteome analysis of barley mesophyll vacuoles revealed the presence of a TMT homolog in the tonoplast fraction (Endler et al., 2006). To date, transport experiments on barley vacuoles have been performed solely with plants grown at approximately room temperature, and it would be interesting to reveal whether cold induction of barley leaves would also lead to an energized glucose transport. TMT activity might be dependent on both translational activation (Figure 5) and posttranslational activation. Therefore, it will be interesting in the future to analyze whether the role of the extraordinarily large, centrally

located loop domain present in all TMT proteins might contribute to this altered mode of transport.

METHODS

Cultivation of Plants and Seedlings

Arabidopsis thaliana plants were grown in a growth chamber in soil at 21°C (day and night), and light was present at 150 μmol·m^{-2}·s^{-1} for 10 h/d (standard growth conditions). For cold stress induction, plants were grown for 6 weeks in the growth chamber and subsequently transferred for 24 h (or 48 h) into a cooled growth chamber (9°C). Drought stress was applied to 5-week-old plants (grown under standard conditions) by withholding water for up to 7 d. For salt stress analysis, surface-sterilized seeds were sown on agar plates containing half-strength MS salts, 0.8% agar, 1% sucrose, 0.05% MES (adjusted to pH 5.7 with KOH), and various NaCl concentrations. Before germination, plates were incubated at 4°C for 2 d in the dark and subsequently transferred to the growth chamber, and growth was continued for 7 d under short-day conditions. To study the effect of sugars on gene expression, wild-type or mutant seedlings were grown for 7 d in liquid half-strength MS medium containing 0.05% MES (adjusted to pH 5.7 with KOH) and glucose, fructose, or sucrose if indicated (Scheible et al., 2004).

Construction of the Sequence Alignment

Multiple alignments of protein sequences were performed with the program ClustalX (Thomson et al., 1994). Transmembrane domains were predicted by the program SOAP in PCgene.

Cloning of the *Arabidopsis TMT1*-GFP and *TMT3*-GFP Constructs and Confocal Microscopy

To construct the TMT1-GFP and TMT3-GFP fusion proteins, we first amplified the entire *TMT1* and *TMT3* cDNAs by PCR using the Pfu-DNA polymerase (Stratagene). The primers used for *TMT1* were the sense primer ML 44 (5′-CCACGCGTCTGAGTCTACTAAAGAG-3′) and the antisense primer ML 45 (5′-AGTTACAAGCTCGAGATCCTTAGAAGG-3′). For the *TMT3* construct, the primers used were the sense primer AW3 (5′-AATCACTGTAATCTAGAAAAAGATGAGGAG-3′) and the antisense primer AW4 (5′-AAGCTGCAGCCTCGAGCTGTTTTGC-3′). The obtained DNA fragments were cleaved with *Xba*I and *Xho*I, respectively, and inserted in-frame in front of the GFP coding region using the vector GFP2 (Kost et al., 1998), leading to the final *TMT1*-GFP and *TMT3*-GFP constructs under the control of a 35S promoter.

Protoplasts isolated from sterile-grown tobacco (*Nicotiana tabacum* cv W38) were transformed with column-purified plasmid DNA (30 μg/0.5 × 10^6 cells) as given (Wendt et al., 2000). After 1 d of incubation at 24°C in the dark, protoplasts in Petri dishes were checked for the presence of green fluorescence by use of a laser-scanning system (LSM510; Carl Zeiss). GFP was excited at 488 nm, and the emission was detected by a photomultiplier through a 505- to 530-nm band-pass filter using an Achroplan 40×/0.75W objective.

Alternatively, cells from an *Arabidopsis* cell suspension culture (Millar et al., 2001) were transiently transformed with column-purified plasmid DNA. The fusion constructs were introduced into *Arabidopsis* protoplasts (Song et al., 2003) by polyethylene glycol–mediated transformation (Jin et al., 2001). Expression of the fusion constructs was monitored at various times after transformation by confocal laser-scanning microscopy using a Leica DM IRE2 microscope with a 63× Plan-Apochromat oil-immersion objective coupled to a TCS-SP2 spectral confocal and multiphoton microscope (Leica Microsystems). Images were processed with the Leica confocal software.

TMT Insertional Mutations

The *Arabidopsis* knockout mutants *tmt1::tDNA1* and *tmt2::tDNA* were kindly provided by the Torrey Mesa Research Institute. A second, independent *tmt1* knockout line (designated *tmt1::tDNA2*) was bought from the GABI-KAT consortium (Max-Planck-Institute), and a third knockout mutant, *tmt3::tDNA*, was provided by the SALK library (Salk Institute for Biological Studies).

To generate double knockout mutants (designated *tmt1-2::tDNA*) lacking *TMT1* and *TMT2* transporter genes, homozygous *tmt1::tDNA1* and homozygous *tmt2::tDNA* mutants were crossed. To obtain a null mutant (*tmt1-2-3::tDNA*) lacking all three functional *TMT* genes, the homozygous double knockout plants were crossed with a homozygous *tmt3::tDNA* mutant.

All knockout lines were analyzed by RT-PCR for the absence of the *TMT1*, *TMT2*, or *TMT3* transcript, respectively, caused by T-DNA insertions. Total leaf RNA from plants grown in the growth chamber was extracted using the RNeasy kit (Qiagen). Subsequently, DNase-treated RNA was transcribed into cDNA via reverse transcriptase (Superscript II; Invitrogen). With the cDNA as template, PCR was performed with 35 cycles of 95°C for 45 s, 58°C for 1 min, and 72°C for 1 min, finishing with an extension at 72°C for 2 min. RT-PCR products were checked on 1% agarose gels.

The following gene-specific primers were used: for *TMT1*, AW31 (5′-GAT-GTTACCGATGAGATGGC-3′) and AW32 (5′-GGAAAATCCCACTCCGA-GTG-3′); for *TMT2*, AW29 (5′-GAGAAGATGAATCGGGACAG-3′) and AW30 (5′-GATGCCTGAGAACTGCTGAAG-3′); and for *TMT3*, AW27 (5′-GATGT-TCAGGCGAGCTTGC-3′) and AW28 (5′-CTCCTGCCTTCCCATCATTC-3′).

cDNA Clones

The full-length *TMT1* cDNA clone (clone No. 8B8T74) derived from the *Arabidopsis* EST project (Newman et al., 1994) was cloned according to standard protocols (Sambrook et al., 1989). For the analysis of sugar-induced molecular responses, we quantified the levels of mRNAs encoding *CAB1* and *NR1*. The full-length cDNAs for *CAB1* (At2g34430) and *NR1* (At1g77760) were amplified using a first-strand cDNA preparation as template, and the amplification products were cloned into the plasmid pBSK and sequenced.

Generation of *TMT-Promoter*–GUS Mutants and Histochemical Localization of GUS Activity

For the generation of the *promoter*–GUS constructs, the binary vector pGPTV (Becker et al., 1992) containing the β-*glucuronidase* (*uidA*) gene from *Escherichia coli* was used. For the generation of the *TMT1*- and *TMT2-promoter*–GUS fusions, a promoter region of ~1.3 kb was cloned upstream of the *GUS* gene. For the generation of the *TMT3-promoter*–GUS fusion, a region of ~850 bp was cloned. The promoter regions of the *TMT* genes (including 30 bp of the coding regions) were amplified by PCR from genomic DNA and were sequenced to check that the correct product was amplified. For amplification of the promoter regions, the following primers were used: for *TMT1*, RW1 (5′-TCTACCCTTTCAATTATC-TATCAATGTTGC-3′) and RW2 (5′-GGCGAGAGCAACCCGGGTCGCT-CCCTTC-3′); for *TMT2*, RW3 (5′-GAGACTGTATGTCGACTTTGGTAC-TCGG-3′) and RW4 (5′-GTTGCGTTATCCCGGCTTGTAACAAGTTG-3′); and for *TMT3*, GUS3-for (5′-CTCTGCTCAAAGGTCGACAAAATTAAC-3′) and GUS3-rev (5′-CTATCGCAGCTGCTAAAGCAAC-3′). After blunt-end ligation of the PCR products in the T7 orientation into the *Sma*I-restricted pBSK vector, the *TMT1* construct was restricted with *Hin*dIII and *Sma*I, the *TMT2* promoter was restricted with *Sal*I and *Sma*I, and the *TMT3* construct was restricted with *Sal*I and *Pvu*II and subsequently inserted in-frame with the *GUS* gene. The resulting constructs were used for *Agrobacterium tumefaciens* transformation. Transformation of *Arabidopsis*

was conducted according to the floral-dip method (Clough and Bent, 1998).

Whole seedlings (grown on MS agar plates) and other tissues from transgenic plants grown on soil under standard growth conditions were collected in ice-cold acetone (90%). After 20 min of incubation at room temperature, samples were stained according to standard protocols (Weigel and Glazebrook, 2002). From each construct, we analyzed 10 to 14 independent lines, and representative results are presented.

Treatment of Leaf Discs for mRNA Quantification, Extraction of Total RNA, and RNA Gel Blot Hybridization

To analyze the effects of sugars on the levels of *CAB1* and *NR1* mRNAs in wild-type and knockout mutant plants, we prepared leaf discs (0.7 cm in diameter) from plants grown for ~4 to 5 weeks in the growth chamber. Three hours after illumination, discs were either transferred directly into liquid nitrogen (controls) or incubated for 24 h in either water or water supplemented with the indicated solutes. Incubation took place in Petri dishes (containing 30 mL of the given solution) in the dark at room temperature (Neuhaus and Stitt, 1989). To prevent anaerobic conditions, samples were incubated on a laboratory shaker at 30 rpm during incubation. Leaf discs used for RNA extraction were frozen and stored in liquid nitrogen until RNA extraction.

The relative accumulation of *TMT* mRNA was analyzed in different *Arabidopsis* tissues prepared from plants grown in the growth chamber. Tissues were harvested and immediately transferred into liquid nitrogen. Total sample RNA was extracted using the Purescript-RNA extraction kit (Gentra Systems). RNA gel blot hybridization was performed as described (Thulke and Conrath, 1998). Labeling of probes was performed using the Ready-To-Go random prime kit (Amersham-Pharmacia). After hybridization, the membranes were washed according to standard procedures, and blots were visualized with a Cyclon phosphor imager (Packard).

Glucose and Fructose Uptake into Isolated Mesophyll Vacuoles and Carbohydrate Quantification

For isolation of intact *Arabidopsis* vacuoles, wild-type or knockout mutant plants were grown for 4 to 5 weeks under standard growth conditions (see above). If not stated otherwise, plants were grown for 2 d at 9°C before vacuole isolation. Isolation of vacuoles was performed as described previously (Frangne et al., 2002; Song et al., 2003). Essentially, mesophyll protoplasts were enriched by enzymatic digestion and centrifugation, and corresponding vacuoles were isolated after mild hypoosmotic treatment of protoplasts. Because enzymatic digestion has to occur for 2.5 h at room temperature, we incubated the resulting protoplasts from cold-adapted plants subsequently for 1 h on ice (to allow a putatively cold-dependent modification of vacuolar glucose transport). We showed elsewhere that *Arabidopsis* vacuoles essentially isolated according to this protocol do not contain other cellular organelles or intact protoplasts (Emmerlich et al., 2003). We checked that intermediate cold incubation of enriched protoplasts, before vacuole isolation (see above), did not alter the purity of the final vacuole preparation (data not shown).

Transport studies of [U-^{14}C]glucose into isolated vacuoles were performed using the silicone oil centrifugation technique (Martinoia and Rentsch, 1992; Emmerlich et al., 2003). Transport was conducted for 10 min (if not stated otherwise) and terminated by centrifugation of intact vacuoles through a layer of silicone oil. Radioactively labeled glucose was given at a concentration of 100 μM (specific radioactivity of 185 kBq/nmol), and Mg^{2+}-ATP (present at a concentration of 1 mM) was given to energize isolated vacuoles.

Sugar extraction from *Arabidopsis* leaves and spectroscopic quantification were performed as described by Quick et al. (1989).

Accession Numbers

GenBank/EMBL accession numbers and Arabidopsis Genome Initiative locus identifiers for the genes mentioned in this article are as follows: *TMT1*, Z50752 and At1g20840;*TMT2*, AJ532570 and At4g35300; *TMT3*, AJ532571 and At3g51490.

Supplemental Data

The following materials are available in the online version of this article.

Supplemental Figure 1. Alignment of the Amino Acid Sequences of the Three *Arabidopsis* TMT Isoforms.

Supplemental Figure 2. Subcellular Localization of a TMT3-GFP Fusion Protein in *Arabidopsis* Suspension Culture Cells.

Supplemental Figure 3. Histochemical *TMT1-Promoter*-GUS Staining at the Cellular Level.

Supplemental Figure 4. PCR Analysis Using Genomic DNA from Wild-Type, *tmt1::tDNA1-*, *tmt1::tDNA2*, *tmt2::tDNA*, *tmt3::tDNA*, *tmt1-2::tDNA*, and *tmt1-2-3::tDNA* Plants.

REFERENCES

Alberdi, M., and Corcuera, L.J. (1991). Cold-acclimation in plants. Phytochemistry **30,** 3177–3184.

ap Rees, T. (1994). Plant physiology. Virtue on both sides. Curr. Biol. **4,** 557–559.

Barrett, M.P., Walmsley, A.R., and Gould, G.W. (1999). Structure and function of facilitative sugar transporters. Curr. Opin. Cell Biol. **11,** 496–502.

Becker, D., Kemper, E., Schell, J., and Masterson, R. (1992). New plant binary vectors with selectable markers located proximal to the left T-DNA border. Plant Mol. Biol. **20,** 1195–1197.

Buchanan, B.B., Gruissem, W., and Jones, R.L. (2000). Biochemistry and Molecular Biology of Plants. (Rockville, MD: American Society of Plant Physiologists).

Bush, D.R. (1999). Sugar transporters in plant biology. Curr. Opin. Plant Biol. **2,** 187–191.

Büttner, M., and Sauer, N. (2000). Monosaccharide transporters in plants: Structure, function and physiology. Biochim. Biophys. Acta **1465,** 263–274.

Cairns, A.J., Pollock, C.J., Gallagher, J.A., and Harrison, J. (2000). Fructans: synthesis and regulation. In Photosynthesis: Physiology and Metabolism, R.C. Leegood, T.D. Sharkey, and C.H. Foyer, eds (Amsterdam, The Netherlands: Kluwer Academic Publishers), pp. 301–320.

Carter, C., Pan, S., Zouhar, J., Avila, E.L., Girke, T., and Raikhel, N.V. (2004). The vegetative vacuole proteome of *Arabidopsis thaliana* reveals predicted and unpredicted proteins. Plant Cell **16,** 3285–3303.

Casu, R.E., Christopher, P.L., Rae, A.L., McIntryre, L., Dimmock, C.M., and Manners, J.M. (2003). Identification of a novel sugar transporter homologue strongly expressed in maturing stem vascular tissues of sugarcane by expressed sequence tag and microarray analysis. Plant Mol. Biol. **52,** 371–386.

Chiou, T.J., and Bush, D.R. (1996). Molecular cloning, immunochemical localization to the vacuole, and expression in transgenic yeast and tobacco of a putative sugar transporter from sugar beet. Plant Physiol. **110,** 511–520.

Clough, S.J., and Bent, A.F. (1998). Floral dip: A simplified method for *Agrobacterium*-mediated transformation of *Arabidopsis thaliana.* Plant J. **16,** 735–743.

Daie, J., and Wilusz, J.E. (1987). Facilitated transport of glucose in isolated phloem segments of celery. Plant Physiol. **84,** 711–715.

Ehrenkranz, J.R., Lewis, N.G., Kahn, C.R., and Roth, J. (2005). Phlorizin: A review. Diabetes Metab. Res. Rev. **21,** 31–38.

Emmerlich, V., Linka, N., Reinhold, T., Hurth, M.A., Traub, M., Martinoia, E., and Neuhaus, H.E. (2003). The plant homolog to the human sodium/dicarboxylic cotransporter is the vacuolar malate carrier. Proc. Natl. Acad. Sci. USA **100,** 11122–11126.

Endler, A., Meyer, S., Schelbert, S., Schneider, T., Weschke, W., Peters, S.W., Keller, F., Baginsky, S., Martinoia, E., and Schmidt, U.G. (2006). Identification of a vacuolar sucrose transporter in barley and Arabidopsis mesophyll cells by a tonoplast proteomic approach. Plant Physiol. **141,** 196–207.

Farré, E.M., Tiessen, A., Roessner, U., Geigenberger, P., Trethewey, R.N., and Willmitzer, L. (2001). Analysis of the compartmentation of glycolytic intermediates, nucleotides, sugars, organic acids, amino acids, and sugar alcohols in potato tubers using a nonaqueous fractionation method. Plant Physiol. **127,** 685–700.

Flügge, U.I. (1999). Phosphate translocators in plastids. Annu. Rev. Plant Physiol. Plant Mol. Biol. **50,** 27–45.

Frangne, N., Eggmann, T., Koblischke, C., Weissenböck, G., Martinoia, E., and Klein, M. (2002). Flavone glucoside uptake into barley mesophyll and Arabidopsis cell culture vacuoles. Energization occurs by H$^+$-antiport and ATP-binding cassette-type mechanisms. Plant Physiol. **128,** 726–733.

Guy, M., Reinhold, L., and Michaeli, D. (1979). Direct evidence for a sugar transport mechanism in isolated vacuoles. Plant Physiol. **64,** 61–64.

Henderson, P.J.F. (1991). Sugar transport proteins. Curr. Opin. Struct. Biol. **1,** 590–601.

Jang, J.C., Leon, P., Zhou, L., and Sheen, J. (1997). Hexokinase as a sugar sensor in higher plants. Plant Cell **9,** 5–19.

Jin, J.B., Kim, Y.A., Kim, S.J., Lee, D.H., Cheong, G.-W., and Hwang, I. (2001). A new dynamin-like protein, ADL6, is involved in trafficking from the *trans*-Golgi network to the central vacuole in Arabidopsis. Plant Cell **13,** 1511–1525.

Kaplan, F., Sung, D.J., and Guy, C.L. (2006). Roles of β-amylase and starch breakdown during temperature stress. Physiol. Plant. **126,** 120–128.

Koch, K.E. (1996). Carbohydrate-modulated gene expression in plants. Annu. Rev. Plant Physiol. Plant Mol. Biol. **47,** 509–540.

Kost, B., Spielhofer, P., and Chua, N.-H. (1998). A GFP-mouse talin fusion protein labels plant actin filaments in vivo and visualizes the actin cytoskeleton in growing pollen tubes. Plant J. **16,** 393–401.

Lalonde, S., Wipf, D., and Frommer, W.B. (2004). Transport mechanisms for organic forms of carbon and nitrogen between source and sink. Annu. Rev. Plant Biol. **55,** 341–372.

Martinoia, E., Kaiser, G., Schramm, M.J., and Heber, U. (1987). Sugar transport across the plasmalemma and the tonoplast of barley mesophyll protoplasts: Evidence for different transport systems. J. Plant Physiol. **131,** 467–478.

Martinoia, E., Massoneau, A., and Frangne, N. (2000). Transport processes of solutes across the vacuolar membrane of higher plants. Plant Cell Physiol. **41,** 1175–1181.

Martinoia, E., and Ratajczak, R. (1997). Transport of organic molecules across the tonoplast. In The Plant Vacuole: Advances in Botany Research, A. Leigh and D. Sanders, eds (London: Academic Press), pp. 365–400.

Martinoia, E., and Rentsch, D. (1992). Uptake of malate and citrate into plant vacuoles. In Transport and Receptor Proteins of Plant Membranes, D.T. Cooke and D.T. Clarkson, eds (New York: Plenum Press), pp. 101–109.

Millar, A.H., Sweetlove, L.J., Giege, P., and Leaver, C.J. (2001). Analysis of the *Arabidopsis* mitochondrial proteome. Plant Physiol. **127,** 1711–1727.

Mueckler, M. (1993). Glucokinase, glucose sensing, and diabetes. Proc. Natl. Acad. Sci. USA **90,** 427–430.

Neuhaus, H.E., and Stitt, M. (1989). Perturbation of photosynthesis in spinach leaf discs by low concentrations of methyl viologen. Planta **179,** 51–60.

Newman, T., De Bruin, F.J., Green, P., Keegstra, K., Kende, H., McIntosh, L., Ohlrogge, J.B., Raikel, N., Sommerville, S., Thomashow, M., Retzel, E., and Sommerville, C.R. (1994). Genes galore: A summary of methods for accessing results from large-scale partial sequencing of anonymous Arabidopsis clones. Plant Physiol. **106,** 1241–1255.

Nittyla, T., Messerli, G., Trevisan, M., Chen, J., Smith, A., and Zeeman, S.C. (2004). A previously unknown maltose transporter essential for starch degradation in leaves. Science **203,** 87–89.

Quick, W.P., Neuhaus, H.E., Feil, R., and Stitt, M. (1989). Fluoride leads to an increase of inorganic pyrophosphate and an inhibition of photosynthetic sucrose synthesis in spinach leaves. Biochim. Biophys. Acta **973,** 263–271.

Rausch, T. (1991). The hexose transporters at the plasma membrane and the tonoplast of higher plants. Physiol. Plant. **82,** 134–142.

Rost, S., Frank, C., and Beck, E. (1997). The chloroplast envelope is permeable for maltose but not for maltodextrins. Biochim. Biophys. Acta **1291,** 221–227.

Ruiz-Medrano, R., Xoconostle-Cazares, B., and Lucas, J. (2001). The phloem as a conduit for inter-organ communication. Curr. Opin. Plant Biol. **4,** 202–209.

Saier, M.H. (2000). A functional-phylogenetic classification system for transmembrane solute transporters. Microbiol. Mol. Biol. Rev. **64,** 345–411.

Sambrook, J., Fritsch, E.F., and Maniatis, T. (1989). Molecular Cloning: A Laboratory Manual. (Cold Spring Harbor, NY: Cold Spring Harbor Laboratory Press).

Schäfer, G., Heber, U., and Heldt, H.W. (1977). Glucose transport into spinach chloroplasts. Plant Physiol. **60,** 286–289.

Scheible, W.R., Morcuende, R., Czechowski, T., Fritz, C., Osuna, D., Palacios-Rojas, N., Schindelasch, D., Thimm, O., Udvardi, M.K., and Stitt, M. (2004). Genome-wide reprogramming of primary and secondary metabolism, protein synthesis, cellular growth processes, and the regulatory infrastructure of Arabidopsis in response to nitrogen. Plant Physiol. **136,** 2483–2499.

Schmetterer, G.R. (1990). Sequence conservation among the glucose transporter from cyanobacterium *Synechocystis* sp. PCC 6803 and mammalian glucose transporters. Plant Mol. Biol. **14,** 697–706.

Shiratake, K., Kanayama, Y., and Yamaki, S. (1997). Characterization of hexose transporter for facilitated diffusion of the tonoplast vesicles from pear fruit. Plant Cell Physiol. **38,** 910–916.

Song, W.Y., Sohn, E.J., Martinoia, E., Lee, Y.J., Yang, Y.Y., Jasinski, M., Forestier, C., Hwang, I., and Lee, Y. (2003). Engineering tolerance and accumulation of lead and cadmium in transgenic plants. Nat. Biotechnol. **21,** 914–919.

Suh, M.C., Samuels, A.L., Jetter, R., Kunst, L., Pollard, M., Ohlrogge, J., and Beisson, F. (2005). Cuticular lipid composition, surface structure, and gene expression in Arabidopsis stem epidermis. Plant Physiol. **139,** 1649–1665.

Thom, M., and Komor, E. (1984). Role of the ATPase of sugarcane vacuoles in energization of the tonoplast. Eur. J. Biochem. **138,** 93–99.

Thomson, J.D., Higgins, D.G., and Gibson, T.J. (1994). CLUSTALW: Improving the sensitivity of progressive multiple alignment through sequence weighting, position-specific gap penalties and weight matrix choice. Nucleic Acids Res. **22,** 4673–4680.

Thulke, O.U., and Conrath, U. (1998). Salicylic acid has a dual role in the activation of defense related genes in parsley. Plant J. **14,** 35–42.

Ward, E.R., Kuhn, C., Tegeder, M., and Frommer, W.B. (1998). Sucrose transport in higher plants. Int. Rev. Cytol. **178,** 41–71.

Weber, A., Servaites, J.C., Geiger, D.E., Koffler, H., Hille, D., Groner, F., Hebbeker, U., and Flügge, U.I. (2000). Identification, purification, and molecular cloning of a putative plastidic glucose translocator. Plant Cell **12,** 787–802.

Weigel, D., and Glazebrook, J. (2002). Arabidopsis. A Laboratory Manual. (Cold Spring Harbor, NY: Cold Spring Harbor Laboratory Press).

Weise, A., Barker, L., Kuhn, C., Lalonde, S., Buschmann, H., Frommer, W.B., and Ward, J.M. (2000). A new subfamily of sucrose transporters, SUT4, with low affinity/high capacity localized in enucleate sieve elements of plants. Plant Cell **12,** 1345–1355.

Wendt, U.K., Wenderoth, I., Tegeler, A., and Von Schaewen, A. (2000). Molecular characterization of a novel glucose-6-phosphate dehydrogenase from potato (*Solanum tuberosum* L.). Plant J. **23,** 723–733.

Weschke, W., Panitz, R., Sauer, N., Wang, Q., Neubohn, B., Weber, H., and Wobus, U. (2000). Sucrose transport into barley seeds: Molecular characterization of two transporters and implications for seed development and starch accumulation. Plant J. **21,** 455–467.

Williams, L.E., Lemoine, R., and Sauer, N. (2000). Sugar transporter in higher plants—A diversity of roles and complex regulation. Trends Plant Sci. **5,** 283–289.

Yano, R., Nakamura, M., Yoneyama, T., and Nishida, I. (2005). Starch-related alpha-glucan/water dikinase is involved in the cold-induced development of freezing tolerance in Arabidopsis. Plant Physiol. **138,** 837–846.

Zimmermann, P., Hirsch-Hoffmann, M., Hennig, L., and Gruissem, W. (2004). GENEVESTIGATOR. Arabidopsis microarray database and analysis toolbox. Plant Physiol. **136,** 2621–2632.